Quenching of single-particle strengths of carbon isotopes [9-12,14-20]C with knockout reactions for incident energies 43–2100 MeV/nucleon[*]

Yi-Ping Xu(许祎萍)[1]   Dan-Yang Pang(庞丹阳)[2]   Cen-Xi Yuan(袁岑溪)[3]   Xiao-Yan Yun(韵小艳)[4†]

[1]School of Nuclear Science and Engineering, North China Electric Power University, Beijing 102206, China
[2]School of Physics, Beihang University, Beijing 100191, China
[3]Sino-French Institute of Nuclear Engineering and Technology, Sun Yat-Sen University, Zhuhai 519082, China
[4]College of Physics and Optoelectronics, Taiyuan University of Technology, Taiyuan 030024, China

Abstract: To study the quenching of single-particle strengths of carbon isotopes, a systematic analysis is performed for [9-12,14-20]C, with single neutron knockout reactions on Be/C targets, within an energy range from approximately 43 to 2100 MeV/nucleon, using the Glauber model. Incident energies do not show any obvious effect on the resulting values across this wide energy range. The extracted quenching factors are found to be strongly dependent on the proton-neutron asymmetry, which is consistent with the recent analysis of knockout reactions but is inconsistent with the systematics of transfer and quasi-free knockout reactions.

Keywords: spectroscopic factors, knockout reactions, reduced single-particle strength, one-neutron removal

I. INTRODUCTION

Spectroscopic factors (SFs) describe the strengths of single-particle states at the Fermi surface of shell closures or quasi-particles and are traditionally considered as a link between studies of nuclear reactions and nuclear structures [1]. SFs extracted from direct nuclear reactions are found to be 30%–40% smaller than shell model predictions [2–4]. Such reduction is generally suggested to originate from nucleon-nucleon (NN) correlations, which cannot be adequately treated in traditional shell model calculations [5, 6]. The quenching of single-particle strength (SPS) is an important topic in nuclear physics (see review [7]). Transfer [8–15], single-nucleon removal [16–24], and quasi-free knockout [25–29] reactions are common probes for the quenching of SPS across a wide region of proton-neutron asymmetry ΔS, which is defined as the difference between the neutron and proton separation energies of the particles concerned, i.e., $\Delta S = S_n - S_p$ for neutron removal and $\Delta S = S_p - S_n$ for proton removal. Experiments using different reactions and/or beam energies are expected to extract consistent nuclear structure information for any nuclei. However, in practice, there are disagreements among these techniques on the degree of the proton-neutron asymmetry dependence of the reduction factors (RFs) of the single-particle strengths, R_s.

A series of systematic studies on the intermediate-energy (mostly between 80−300 MeV/nucleon) single nucleon knockout measurements of various radioactive light nuclei on Be/C targets [17, 19, 24] show a strong dependence of the reduction factors on ΔS. The situation of single-proton and single-neutron removal reactions over long isotopic chains of medium-mass nuclei seems to be different [22]. R_s for the single-neutron removal on tin isotopes does not show any clear dependence with ΔS, but for the single-neutron removal on same nuclei, R_s shows a clear decrease with the proton-neutron asymmetry, similar to that in Ref. [24]. In contrast, for transfer reactions [10, 13–15] and $(p,2p)$ and (p,pn) reactions [25, 26, 28, 29], there is so far no obvious evidence that R_s depends on ΔS. It is still an open question why the proton-neutron asymmetry dependence of the RFs differs systematically for different reactions. A similar discrepancy exists in structure theoretical calculation [25, 26, 30–33].

The Glauber model is widely used in previous systematic studies on knockout reactions [17, 19, 20, 23, 24]. However, the incident energy being large enough is crucial for the validity of the eikonal and sudden approximations, which form the basis of the Glauber model. RFs extracted from knockout reactions with a variety of incident energies can provide significant information to im-

prove the Glauber model in its incident-energy-dependent part [23]. In our previous study [20], we analyzed the single neutron removal cross sections pf the neutron-rich $^{15\text{-}19}$C isotopes on Be/C targets at incident energies between 50 –900 MeV/nucleon. No strong incident energy dependence was found in the RFs of these nuclei within this energy range. In this study, we carry out a systematic analysis of available measurements of one-neutron knockout data for carbon isotopes $^{9\text{-}12,14\text{-}20}$C. With the inclusion of new data measured at higher energies and results with proton-rich carbon isotopes, our goals are (i) to investigate the incident energy dependence in R_s throughout a wider energy region up to 2100 MeV/nucleon and (ii) to explore the proton-neutron asymmetry dependence of quenching of single neutron strengths for both proton-rich and neutron-rich carbon isotopes. The ΔS values range from –26.6 to 12.9 MeV for these nuclei.

II. ONE NEUTRON REMOVAL REACTIONS AND THE RFs

For knockout reactions, the experimental one-neutron removal cross sections, $\sigma_{-1n}^{\text{exp}}$, are usually inclusive, that is, contributions from all the bound excited states of the knockout residues were included in the measured data. Therefore, the theoretical one-neutron removal cross sections σ_{-1n}^{th} were calculated as sums of the single-particle removal cross sections [18]:

$$\sigma_{-1n}^{\text{th}} = \sum_{nlj}\left[\frac{A}{A-1}\right]^{N_{nl}} C^2 S(J^\pi, nlj)\sigma_{\text{sp}}(nlj, S_n), \quad (1)$$

where $C^2 S(J^\pi, nlj)$ are the shell model SFs, which depend on the spin-parties of the core states, J^π, and the quantum numbers of the single-particle states of the removed nucleon, nlj. The factors $\left[\frac{A}{A-1}\right]^{N_{nl}}$ are for the center-of-mass corrections to the shell model SFs, where N_{nl} is the number of the oscillator quanta associated with the major shell of the removed particle, which depends on the node number n and orbital angular momentum l, and A is the mass number of the composite nucleus [9, 22]. The single-particle cross sections, σ_{sp}, include contributions from both the stripping and diffraction dissociation mechanisms [34], that is, $\sigma_{\text{sp}} = \sigma_{\text{dif}} + \sigma_{\text{str}}$.

In the Glauber theory, the σth calculation requires (i) the final-states spectra and shell model SFs, (ii) the core- and valence-target elastic S-matrices, and (iii) the removed-neutron radial wave-function associated with each bound state of the core nucleus. For (i), the shell model spectroscopic factors $C^2 S(J^\pi, nlj)$ are obtained from large-basis shell model (LB-SM) calculations with the code OXBASH, using the interaction YSOX [35]. For (ii), with the optical limit of the Glauber theory and the

$t\rho\rho$ approximation, we need the nucleon-nucleon (NN) scattering amplitudes, and the nucleon density distributions of the core nucleus and the valence nucleon, and the target nuclei. To be consistent with our previous analyses of knockout reactions [20], the nucleon density distributions are also obtained with Hartree-Fock calculations based on the Skyrme SkX interaction [36], except that a two-parameter Fermi density with $\rho_0 = 0.194$ fm^{-3}, $c = 2.214$ fm, and $a = 0.425$ fm is used for ^{12}C.

There have been different parametrizations of the NN scattering amplitudes. We used the parameters of Horiuchi *et al.* [37] in our previous work, which covers an energy range from 30 to 1000 MeV/nucleon. A new measurement at 1.6 GeV/nucleon is performed for the carbon isotopes $^{10\text{-}12}$C(-n) at the GSI Helmholtzzentrum für Schwerionen-forschung, Darmstadt, Germany [38]. For this reason, we use the new global parameter set developed by Tran *et al.* [39], which is applicable to reaction cross section σ_R measurements at incident energies from 10 to 2100 MeV/nucleon.

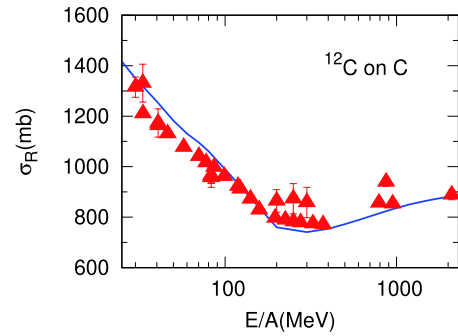As shown in Fig. 1, our calculations show reasonable

Fig. 1. (color online) Comparison of total reaction cross sections of ^{12}C on carbon target at various incident energies between theoretical and experimental results. The experimental data(triangles) are taken from Refs. [41– 46]. The solid curve are theoretical results with the parameters.
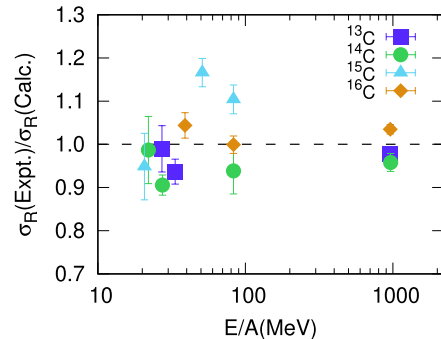

Fig. 2. (color online) Ratios of experimental to theoretical total cross sections of $^{13\text{-}16}$C on carbon target at various incident energies. The experimental data are taken from Refs. [44–46].

agreement with the experimental σ_R for reactions of ^{12}C on carbon targets in the whole energy range. Figure 2 is a plot of the discrepancy between the data and the calculation for other carbon isotopes: $^{13\text{-}16}$C. The discrepancies are below 10% except for ^{15}C, which reaches almost 20%. All our calculations are performed with the computer code MOMDIS [40].

For (iii), the single-neutron wave functions are obtained by using the Woods-Saxon (WS) potential geometry with a radius parameter $r_0 = 1.25$ fm and a diffuseness $a_0 = 0.7$ fm, which are the same as those adopted in analysis of knockout reactions in, e.g., Refs. [18, 20, 23]. The depths of the WS potentials are adjusted to reproduce the experimental separation energy, and the excitation energy of each final state was taken into account. All above data on nuclei used in theoretical calculations are listed in Table 1.

The RFs in knockout reactions, R_s, are defined as the ratio between the experimental and theoretical one-neutron removal cross sections, that is, $R_s = \sigma_{\exp}/\sigma_{\text{th}}$. Once the above parameters are determined, the theoretical one-neutron removal cross sections σ_{th} for the carbon isotopes with carbon and beryllium targets at various energies can be calculated. For R_s values determined by more than one measurement, we define an averaged reduction factor $\overline{R_s}$, which is a weighted mean of the R_s from each measurement. The weighting factor is chosen to be the reciprocal of the square of ΔR_s:

$$w_i = \left[\frac{1}{(\Delta R_s)_i}\right]^2, \tag{2}$$

$$\overline{R_s} = \frac{\sum_i (R_s)_i w_i}{\sum_i w_i}, \tag{3}$$

$$\overline{\Delta R_s} = \frac{1}{\sqrt{\sum_i w_i}}. \tag{4}$$

Following the definition in Ref. [18], the effective proton-neutron asymmetry ΔS^{eff} is given by

$$\Delta S^{\text{eff}}(A) = S_n(A) - S_p(A) + \overline{E}_f(A-1), \tag{5}$$

where S_n and S_p are the neutron and proton separation energies in the ground state of the target nucleus. $\overline{E}_f$ is the effective final state excitation energy, which is obtained by weighting the excitation energy E^* of each state by the corresponding one-neutron removal cross sections. The results are listed in Table 2 together with the corresponding experimental removal cross sections.

III. RESULTS AND DISCUSSIONS

The reduction factors as a function of the incident en-

Table 1. The nuclei information used in theoretical calculations, including ground-state proton-neutron asymmetry ΔS, bound states of the core nuclei, E_x and J^π, and their associate single-particle states, nlj of the valence nucleon and single-particle spectroscopic factors (C^2S) as results of shell model calculations used in one neutron removal cross section calculation of the carbon isotopes.

Reaction	ΔS /MeV	E_x /MeV	J^π	nlj	C^2S
$(^9$C, ^{8}C$)$	12.93	0.000	0^+	$0p_{3/2}$	0.868
$(^{10}$C, ^{9}C$)$	17.28	0.000	$\frac{3}{2}^-$	$0p_{3/2}$	1.741
$(^{11}$C, ^{10}C$)$	4.43	0.000	0^+	$0p_{3/2}$	0.423
		3.354	$\frac{3}{2}^-$	$0p_{3/2}$	1.567
$(^{12}$C, ^{11}C$)$	2.76	0.000	$\frac{3}{2}^-$	$0p_{3/2}$	2.789
		2.000	$\frac{1}{2}^-$	$0p_{1/2}$	0.616
		4.804	$\frac{3}{2}^-$	$0p_{3/2}$	0.385
$(^{14}$C, ^{13}C$)$	−12.66	0.000	$\frac{1}{2}^-$	$0p_{1/2}$	1.580
		3.089	$\frac{1}{2}^+$	$1s_{1/2}$	0.021
		3.685	$\frac{3}{2}^-$	$0p_{3/2}$	2.031
		3.854	$\frac{5}{2}^+$	$0d_{5/2}$	0.118
$(^{15}$C, ^{14}C$)$	−19.86	0.000	0^+	$1s_{1/2}$	0.953
		6.094	1^-	$0p_{3/2}$	0.086
				$0p_{1/2}$	1.015
		6.589	0^+	$1s_{1/2}$	0.007
		6.903	0^-	$0p_{1/2}$	0.410
		7.012	2^+	$0d_{5/2}$	0.004
		7.341	2^-	$0p_{3/2}$	0.006
$(^{16}$C, ^{15}C$)$	−18.30	0.000	$\frac{1}{2}^+$	$1s_{1/2}$	0.734
		0.740	$\frac{5}{2}^+$	$0d_{5/2}$	1.167
$(^{17}$C, ^{16}C$)$	−22.64	0.000	0^+	$0d_{3/2}$	0.032
		1.766	2^+	$1s_{1/2}$	0.149
				$0d_{5/2}$	1.301
				$0d_{3/2}$	0.034
		3.987	2^+	$1s_{1/2}$	0.275
				$0d_{5/2}$	0.077
				$0d_{3/2}$	0.024
		4.143	4^+	$0d_{5/2}$	0.330
$(^{18}$C, ^{17}C$)$	−21.91	0.000	$\frac{3}{2}^+$	$0d_{3/2}$	0.088
		0.217	$\frac{1}{2}^+$	$1s_{1/2}$	0.803
		0.332	$\frac{5}{2}^+$	$0d_{5/2}$	2.734
$(^{19}$C, ^{18}C$)$	−26.09	0.000	0^+	$1s_{1/2}$	0.502
		1.589	2^+	$0d_{5/2}$	0.585
				$0d_{3/2}$	0.003
		2.515	2^+	$0d_{5/2}$	0.038
				$0d_{3/2}$	0.079
		3.972	3^+	$0d_{5/2}$	1.682
			2^+	$0d_{5/2}$	0.793
				$0d_{3/2}$	0.008
$(^{20}$C, ^{19}C$)$	−26.58	0.000	0^+	$1s_{1/2}$	1.201

Table 2. Results of experimental ($\sigma_{-1n}^{\exp}$) and theoretical inclusive one-neutron removal cross sections (σ_{-1n}^{th}) for carbon isotopes at different incident energies, the corresponding effective proton-neutron asymmetry ΔS^{eff}, and quenching factors of the neutron spectroscopic factors.

| Reaction	Target	E_{in}/(MeV/u)	ΔS^{eff}/MeV	$\sigma_{-1n}^{\exp}$/mb	σ_{-1n}^{th}/mb	R_s
(^{9}C, ^{8}C)	^{9}Be	66.8 [21]	12.93	3.93±0.88	33.39	0.118±0.026
(^{10}C, ^{9}C)	^{12}C	120 [47]	17.28	23.4±11	62.53	0.374±0.176
	^{9}Be	120 [47]	17.28	27.4±13	55.29	0.496±0.235
	^{9}Be	1670 [38]	17.28	20.21±0.28	48.42	0.417±0.006
Average			17.30			0.417±0.006
(^{11}C, ^{10}C)	^{9}Be	1670 [38]	7.02	24.44±0.21	58.17	0.420±0.004
(^{12}C, ^{11}C)	^{12}C	94.6 [48]	3.54	53±22	125.35	0.423±0.176
	^{12}C	240 [49]	3.54	60.51±11.08	100.49	0.602±0.110
	^{12}C	250 [50]	3.54	55.97±4.06	100.20	0.559±0.041
	^{12}C	600 [51]	3.54	53.6±0.804	97.32	0.551±0.008
	^{12}C	1050 [52]	3.53	44.7±2.8	96.75	0.462±0.029
	^{9}Be	1670 [38]	3.54	49.44±0.88	96.07	0.515±0.009
	^{12}C	2100 [52]	3.53	46.5±2.3	96.02	0.484±0.024
Average			3.54			0.529±0.006
(^{14}C, ^{13}C)	^{12}C	67 [53]	−10.70	65±4	136.85	0.475±0.029
	^{12}C	83 [54]	−10.69	67±14	133.28	0.503±0.105
	^{12}C	235 [23]	−10.69	80±7	105.43	0.759±0.066
	^{9}Be	700 [55]	−10.69	62±9	100.32	0.618±0.090
Average			−10.70			0.528±0.025
(^{15}C, ^{14}C)	^{12}C	54 [34]	−18.03	137±16	211.42	0.648±0.076
	^{12}C	62 [53]	−17.98	159±15	201.81	0.788±0.074
	^{12}C	83 [54]	−17.87	146±23	182.59	0.800±0.126
	^{9}Be	103 [56]	−17.69	140.2±4.6	141.23	0.993±0.033
	^{12}C	237 [23]	−17.71	108±11	134.02	0.806±0.082
	^{9}Be	700 [55]	−17.72	148±23	128.59	1.151±0.179
Average			−17.77			0.907±0.025
(^{16}C, ^{15}C)	^{12}C	55 [53]	−17.94	65±6	112.07	0.580±0.054
	^{9}Be	62 [57]	−17.93	77±9	95.19	0.809±0.095
	^{9}Be	75 [58]	−17.93	81±7	90.98	0.890±0.077
	^{12}C	83 [59]	−17.93	65±15	102.43	0.635±0.146
	^{12}C	239 [23]	−17.92	83±8	80.19	1.035±0.100
	^{9}Be	700 [55]	−17.92	63±19	77.23	0.816±0.246
Average			−17.93			0.744±0.036
(^{17}C, ^{16}C)	^{12}C	49 [53]	−20.22	84±9	129.97	0.646±0.069
	^{9}Be	62 [57]	−20.21	115±14	108.30	1.062±0.129
	^{12}C	79 [18]	−20.21	116±18	117.58	0.987±0.153
	^{9}Be	700 [55]	−20.28	72±19	99.34	0.725±0.191
	^{12}C	904 [52]	−20.21	129±22	96.97	1.330±0.227
Average			−20.22			0.800±0.053
(^{18}C, ^{17}C)	^{12}C	43 [53]	−21.62	115±18	181.22	0.635±0.099
	^{12}C	80 [18]	−21.62	155±24	162.91	0.951±0.147
	^{9}Be	700 [55]	−21.62	80±14	124.50	0.643±0.112
Average			−21.62			0.702±0.066
(^{19}C, ^{18}C)	^{9}Be	57 [57]	−24.00	264±80	192.27	1.373±0.416
	^{9}Be	64 [18]	−23.96	226±65	186.05	1.215±0.349
	^{9}Be	88 [60]	−23.87	105±17	169.51	0.619±0.100
	^{12}C	243 [61]	−23.82	163±12	152.39	1.070±0.079
	^{9}Be	700 [55]	−23.83	122±32	147.22	0.829±0.217
	^{12}C	910 [52]	−23.95	233±51	165.44	1.408±0.308
Average			−23.85			0.928±0.057
(^{20}C, ^{19}C)	^{12}C	241 [61]	−26.58	58±5	60.87	0.953±0.082
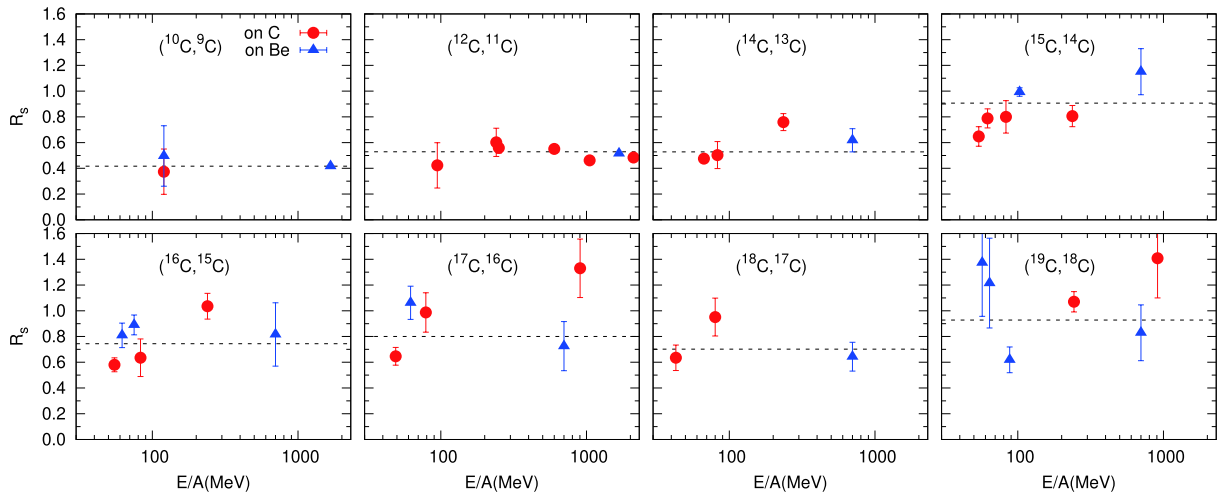
Fig. 3. (color online) Reduction factors of the single neutron spectroscopic factors of the carbon isotopes extracted from experimental data at various incident energies. The dashed lines represent the weighted average R_s values.
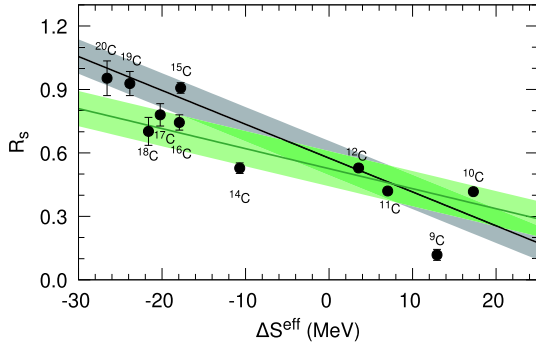

Fig. 4. (color online) Averaged reduction factors from the reactions analyzed in this work (symbols). The green and grey bars represent the linear dependence of R_s on the ΔS^{eff} values fitted assuming a free or a fixed slope, respectively. See the text for details.

ergy for each of the carbon isotopes are shown in Fig. 3. The R_s for the single-neutron removal still does not show clear dependence with the incident energy, except for ^{15}C, although some measurements at higher beam energies are included. Note that the R_s values scatter considerably for ^{15,17,19}C, which can be due to the large uncertainties in the experimental cross sections. Therefore, more precise measurements for these nuclei are expected. Interestingly, ^{15,19}C are two examples of neutron halo nucleus. The situation concerning a halo structure in ^{17}C is rather contentious. Maybe it is a halo-like nucleus or neutron skin nucleus. These phenomena may be related to the complex structure of these nuclei. A more detailed study of the halo structure of ^{15,17,19}C with different reaction or structure models is needed to clarify it.

The averaged reduction factor $\overline{R_s}$ are fitted by a linear function on the ΔS^{eff} values, $\overline{R_s} = a \times \Delta S^{\text{eff}} + b$. These fittings are made by assuming either (i) $a = -0.016$, which is the same as that in Ref. [24], and b to vary freely, or

(ii) both a and b to vary freely. The results are depicted in Fig. 4, where the widths of these bars represent their corresponding χ^2. As can be seen, the averaged reduction factor shows a clear decrease with the proton-neutron asymmetry, although the free slope is weaker than the one observed in Ref. [24].

Slope values for other systematic studies are provided in Table 3, as well as studied nuclei and the proton-neutron asymmetry energy range, including results from single-nucleon removal, transfer, $(e,e'p)$, and quasi-free knockout reactions. Figure 5 shows the slope parameters from linear fits of reduction factors for different reactions. The horizontal line segment represents the slope via a linear fit of all data from a certain compilation, and the band corresponds to fitting results to different sets of the same experimental data depending on the choice of theoretical models and parameters. The blue diamond stands for results from this work. The blue horizontal bands correspond to reduction factors of knockout reactions using only Sn isotopes, with the results from single-neutron removal on the left [22, 62, 63] and those from single-proton removal on the right [22, 62, 63]. The result from a recent compilation of light nuclei knockout measurements by Tostevin [24] is represented by the blue segment. The red line and bands correspond to the linear fit values taken from deuteron single nucleon transfer measurements, including the analyses on Ar/Ca isotopes (left red line) [15] and oxygen isotopes (middle red band) [11, 13], respectively, and a compilation by our previous work (right red band) [14]. The green line corresponds to the slope from a linear fit using $(e,e'p)$ data [8]. The purple lines and bands correspond to separate analyses of $(p,2p)$ and (p,pn) measurements on oxygen, carbon, and nitrogen targets. The $(p,2p)$ and (p,pn) results from Holl et al. [29], Gómez-Ramos et al. [26], Phuc et al. [28], and Atar et al. [25] are shown in order from left to right. As

Table 3. The slope parameters of reduction factors fitted by different experimental results.

| Reactions	Isotopes	ΔS/MeV	Slope/MeV^{-1}	Data Sets	Ref.
Knockout(-*n*)	$^{9\text{-}12,14\text{-}20}$C	$-26.6\sim17.3$	-0.0095	43	present
Knockout(-*n*)	$^{104,110,113\text{-}115,121\text{-}123,126\text{-}135}$Sn	$-14.0\sim8.4$	$0.0091\sim0.013$	18	[22, 62, 63]
Knockout(-*p*)	$^{104,110,112,120,124,129\text{-}133}$Sn	$-8.4\sim13.3$	$-0.027\sim-0.024$	10	[22, 62, 63]
Knockout(-*n*)/(-*p*)	^{9}Li, ^{10}Be, ^{8}B, ^{9,10,12,15,16,19,20}C, ^{14,16,24}O, ^{25}F, ^{29,30}Ne, ^{33}Na,^{22,28}Mg, ^{24,34,36,38,40}Si, ^{43}P, ^{28,36,44}S, ^{32,34,46}Ar, ^{36}Ca, ^{57}Ni,^{71}Co	$-26.6\sim20.5$	-0.016	48	[19, 24]
(*p*,*d*)/(*d*,*p*)	$^{34,36\text{-}41,46}$Ar, $^{40\text{-}45,47\text{-}49}$Ca	$-11.3\sim12.4$	0.0014	33	[15]
(*d*,*t*)/(*d*,^{3}He)	^{14,16,18}O	$-18.6\sim18.6$	$-0.0076\sim0.0024$	10	[11, 13]
(*p*,*d*)	^{8}He,^{12,14}C, ^{14,16,18}O, ^{22}Ne, ^{26}Mg, ^{28,30}Si, ^{34}S, ^{34,36,38,46}Ar, ^{40,42,44,48}Ca, ^{46}Ti, ^{56}Ni	$-22.3\sim18.6$	$-0.0004\sim0.0023$	103	[14]
(*e*,*e*′*p*)	^{7}Li, ^{12}C, ^{16}O, ^{30}Si, ^{31}P, ^{40,48}Ca, ^{51}V, ^{90}Zr, ^{208}Pb	$-7.3\sim5.9$	0.0043	10	[8]
(*p*,2*p*)/(*p*,*pn*)	$^{10\text{-}12}$C, ^{21}N, $^{14,16,17,21\text{-}23}$O	$-22.3\sim22.3$	-0.0060	15	[29]
(*p*,2*p*)/(*p*,*pn*)	^{12}C, ^{21}N, $^{13\text{-}18,21\text{-}23}$O	$-22.3\sim22.3$	$-0.0031\sim0.0004$	16	[26]
(*p*,2*p*)/(*p*,*pn*)	$^{10\text{-}12}$C, ^{21}N, $^{13\text{-}18,21\text{-}23}$O	$-22.3\sim22.3$	-0.0026	18	[28]
(*p*,2*p*)	^{14,16,17,21,23}O	$-18.6\sim22.3$	-0.0033	5	[25]
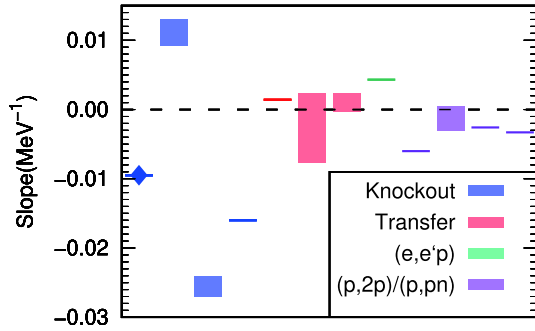
Fig. 5. (color online) A summary of reduction-factor slope parameters across different reactions. The blue lines and bands are slope values of knockout reactions extracted from my work and Refs. [19, 22, 24, 62, 63], respectively. The red line and bands correspond to the slope values taken from single nucleon transfer reactions using data from Refs. [11, 13-15], respectively. The green line stands for the slope fitted by (*e*,*e*′*p*) data [8]. The purple lines and bands represent the (*p*,2*p*)/(*p*,*pn*) results from Ref. [25, 26, 28, 29]. See the text for details, and the slope values are provided in Table 3 with corresponding citations.

can be seen, except for (*e*,*e*′*p*) reactions, which do not cover a wide asymmetry range, transfer reactions and (*p*,2*p*)/(*p*,*pn*) do not exhibit clear dependence on proton-neutron asymmetry, as observed in knockout reactions on beryllium and carbon targets. Ref. [14] has suggested that the systematical discrepancy between transfer and knockout reactions is not due to the exclusive or inclusive treatment of the experimental data. This discrepancy among the different experimental probes may be due to different reaction descriptions bringing different approximation schemes, model inputs, and uncertainties. Understanding the discrepancy is a key issue in nuclear physics to be solved in the near future, in view of the goal of obtaining consistent nuclear structure information.

IV. SUMMARY

In summary, we performed a systematic analysis of the one-neutron removal cross sections of the carbon isotopes, $^{9\text{-}12,14\text{-}20}$C, within a wide energy range from approximately 43 to 2100 MeV/nucleon, using the Glauber model. Our results suggest that a clear proton-neutron asymmetry dependence is seen over a wide range of ΔS values, which is consistent with the earlier systematic studies on knockout reactions [17, 19, 24]. Our results also show no strong incident energy dependence in the R_s values of these nuclei within the wide energy range studied. Agreement between this work and our previous work from Ref. [20] indicates that the incident energy dependence plays a minor role in the study of quenching factors.

References

[1]   N. K. Glendenning. *Direct Nuclear Reactions*. World Scientific, Singapore, 2004
[2]   J. W. A. denHerder, H. P. Blok, E. Jans *et al.*, *Nucl. Phys. A* **490**(3), 507-555 (1988)
[3]   L. Lapikas, *Nuclear Physics A* **553**, 297-308 (1993)
[4]   G. J. Kramer, H. P. Blok, and L. Lapikas, *Nucl. Phys. A* **679**(3), 267-286 (2001)
[5]   Vijay R. Pandharipande, Ingo Sick, and Peter K. A. deWitt Huberts, *Rev. Mod. Phys.* **69**, 981-991 (1997)
[6]   W. H. Dickhoff and C. Barbieri, *Progress in Particle and Nuclear Physics* **52**(2), 377-496 (2004)
[7]   T. Aumann, C. Barbieri, and D. Bazin *et al.*, *Progress in*

Particle and Nuclear Physics **118**, 103847 (2021)

[8] Jenny Lee, J. A. Tostevin, and B. A. Brown *et al*., *Phys. Rev. C* **73**, 044608 (2006)

[9] M. B. Tsang, Jenny Lee, and S. C. Su, *et al*., *Phys. Rev. Lett.* **102**, 062501 (2009)

[10] Jenny Lee, M. B. Tsang, and D. Bazin, *et al*., *Phys. Rev. Lett.* **104**, 112701 (2010)

[11] F. Flavigny, A. Gillibert, and L. Nalpas, *et al*., *Phys. Rev. Lett.* **110**, 122503 (2013)

[12] B. P. Kay, J. P. Schiffer, and S. J. Freeman, *Phys. Rev. Lett.* **111**, 242502 (2013)

[13] F. Flavigny, N. Keeley, A. Gillibert *et al*., *Phys. Rev. C* **97**, 034601 (2018)

[14] Y. P. Xu, D. Y. Pang, X. Y. Yun *et al*., *Phys. Lett. B* **790**, 308-313 (2019)

[15] J. Manfredi, J. Lee, A. M. Rogers *et al*., *Phys. Rev. C* **104**, 024608 (2021)

[16] A. Gade, D. Bazin, B. A. Brown *et al*., *Phys. Rev. Lett.* **93**, 042501 (2004)

[17] A. Gade, P. Adrich, D. Bazin *et al*., *Phys. Rev. C* **77**, 044306 (2008)

[18] E. C. Simpson and J. A. Tostevin, *Phys. Rev. C* **79**, 024616 (2009)

[19] J. A. Tostevin and A. Gade, *Phys. Rev. C* **90**, 057602 (2014)

[20] Chao Wen, Yi-Ping Xu, Dan-Yang Pang *et al*. *Quenching of neutron spectroscopic factors of radioactive carbon isotopes with knockout reactions within a wide energy range*. **41**(5): 054104, may 2017

[21] R. J. Charity, L. G. Sobotka, and J. A. Tostevin, *Phys. Rev. C* **102**, 044614 (2020)

[22] J. Díaz-Cortés, J. Benlliure, J. L. Rodríguez-Sánchez *et al*., *Phys. Lett. B* **811**, 135962 (2020)

[23] Y. Z. Sun, S. T. Wang, Z. Y. Sun *et al*., *Phys. Rev. C* **104**, 014310 (2021)

[24] J. A. Tostevin and A. Gade, *Phys. Rev. C* **103**, 054610 (2021)

[25] L. Atar, S. Paschalis, C. Barbieri *et al*., *Phys. Rev. Lett.* **120**, 052501 (2018)

[26] M. Gómez-Ramos and A.M. Moro, *Phys. Lett. B* **785**, 511-516 (2018)

[27] Shoichiro Kawase, Tomohiro Uesaka, Tsz Leung Tang *et al*., *Progress of Theoretical and Experimental Physics* **2018**(2), 02 (2018)

[28] Nguyen Tri Toan Phuc, Kazuki Yoshida, and Kazuyuki Ogata, *Phys. Rev. C* **100**, 064604 (2019)

[29] M. Holl, V. Panin, H. Alvarez-Pol *et al*., *Phys. Lett. B* **795**, 682-688 (2019)

[30] C. Barbieri, *Phys. Rev. Lett.* **103**, 202502 (2009)

[31] N. K. Timofeyuk, *Phys. Rev. Lett.* **103**, 242501 (2009)

[32] A. Cipollone, C. Barbieri, and P. Navrátil, *Phys. Rev. C* **92**, 014306 (2015)

[33] S. Paschalis, M. Petri, A. O. Macchiavelli *et al*., *Phys. Lett. B* **800**, 135110 (2020)

[34] J. A. Tostevin, D. Bazin, B. A. Brown *et al*., *Phys. Rev. C* **66**, 024607 (2002)

[35] Cenxi Yuan, Toshio Suzuki, akaharu Otsuka *et al*., *Phys. Rev. C* **85**, 064324 (2012)

[36] B. Alex Brown, *Phys. Rev. C* **58**, 220-231 (1998)

[37] W. Horiuchi, Y. Suzuki, B. Abu-Ibrahim *et al*., *Phys. Rev. C* **75**, 044607 (2007)

[38] Steffen Erich Schlemme. *Nucleon-knockout Reactions from Neutron-deficient Carbon Isotopes and Characterization of a Particle Detector Combination for the Super-FRS at FAIR*. PhD thesis, Technische Universität, Darmstadt, 2019

[39] D. T. Tran, H. J. Ong, T. T. Nguyen *et al*., *Phys. Rev. C* **94**, 064604 (2016)

[40] C. A. Bertulani and A. Gade, *Computer Physics Communications* **175**(5), 372-380 (2006)

[41] J. Jaros, A. Wagner, L. Anderson *et al*., *Phys. Rev. C* **18**, 2273-2292 (1978)

[42] C. Perrin, S. Kox, N. Longequeue *et al*., *Phys. Rev. Lett.* **49**, 1905-1909 (1982)

[43] S. Kox, A. Gamp, C. Perrin *et al*., *Phys. Rev. C* **35**, 1678-1691 (1987)

[44] D. Q. Fang, W. Q. Shen, J. Feng *et al*., *Phys. Rev. C* **61**, 064311 (2000)

[45] H. Y. Zhang, W. Q. Shen, Z. Z. Ren *et al*., *Nucl. Phys. A* **707**(3), 303-324 (2002)

[46] T. Zheng, T. Yamaguchi, A. Ozawa *et al*., *Nucl. Phys. A* **709**(1), 103-118 (2002)

[47] G. F. Grinyer, D. Bazin, A. Gade *et al*., *Phys. Rev. C* **86**, 024315 (2012)

[48] J. Dudouet, D. Juliani, M. Labalme *et al*., *Phys. Rev. C* **88**, 024606 (2013)

[49] Yazhou SUN, Yixuan ZHAO, Shuya JIN *et al*., *Nucl. Phys. Rev.* **37**, 742 (2020)

[50] J. M. Kidd, P. J. Lindstrom, H. J. Crawford *et al*., *Phys. Rev. C* **37**, 2613-2623 (1988)

[51] W. R. Webber, J. C. Kish, and D. A. Schrier, *Phys. Rev. C* **41**, 547-565 (1990)

[52] Baumann T. Geissel H *et al*., *The European Physical Journal A* **10**, 49-56 (2001)

[53] E. Sauvan, F. Carstoiu, N. A. Orr *et al*., *Phys. Rev. C* **69**, 044603 (2004)

[54] D. Q. Fang, T. Yamaguchi, T. Zheng *et al*., *Phys. Rev. C* **69**, 034613 (2004)

[55] C. Rodríguez-Tajes, H. 8lvarez-Pol, T. Aumann *et al*., *Phys. Rev. C* **82**, 024305 (2010)

[56] J. R. Terry, D. Bazin, B. A. Brown *et al*., *Phys. Rev. C* **69**, 054306 (2004)

[57] V. Maddalena, T. Aumann, D. Bazin *et al*., *Phys. Rev. C* **63**, 024613 (2001)

[58] F. Flavigny, A. Obertelli, A. Bonaccorso *et al*., *Phys. Rev. Lett.* **108**, 252501 (2012)

[59] T. Yamaguchi, T. Zheng, A. Ozawa *et al*., *Nucl. Phys. A* **724**(1), 3-13 (2003)

[60] D. Bazin, W. Benenson, B. A. Brown *et al*., *Phys. Rev. C* **57**, 2156-2164 (1998)

[61] N. Kobayashi, T. Nakamura, J. A. Tostevin *et al*., *Phys. Rev. C* **86**, 054604 (2012)

[62] L. Audirac, A. Obertelli, P. Doornenbal *et al*., *Phys. Rev. C* **88**, 041602 (2013)

[63] J. L. Rodríguez-Sánchez, J. Benlliure, C. A. Bertulani *et al*., *Phys. Rev. C* **96**, 034303 (2017)